Journal of Colloid and Interface Science 564 (2020) 1–7

Contents lists available at ScienceDirect

Journal of Colloid and Interface Science

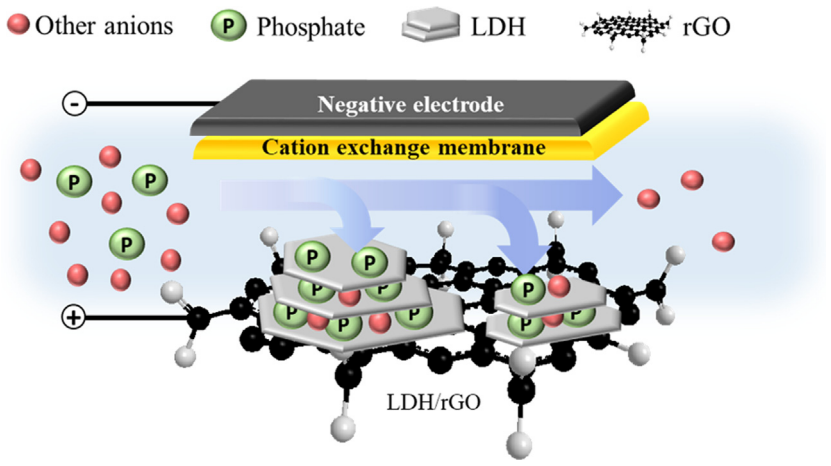
journal homepage: www.elsevier.com/locate/jcis

Selective phosphate removal using layered double hydroxide/reduced graphene oxide (LDH/rGO) composite electrode in capacitive deionization

Sung Pil Hong [a], Hansun Yoon [a], Jaehan Lee [b], Choonsoo Kim [c], Seoni Kim [a], Jiho Lee [a], Changha Lee [a], Jeyong Yoon [a,d,*]

[a] School of Chemical and Biological Engineering and Institute of Chemical Processes (ICP), Seoul National University, Seoul 08826, Republic of Korea
[b] Department of Biological and Chemical Engineering, College of Science and Technology, Hongik University, Sejong-si 30016, Republic of Korea
[c] Department of Environmental Engineering and Institute of Energy/Environment Convergence Technologies, Kongju National University, 1223-24, Cheonan-daero, Cheonan-si 31080, Republic of Korea
[d] Korea Environment Institute, 370 Sicheong-daero, Sejong-si 30147,Republic of Korea

GRAPHICAL ABSTRACT



ARTICLE INFO

Article history:
Received 8 October 2019
Revised 7 December 2019
Accepted 16 December 2019
Available online 17 December 2019

Keywords:
Water treatment
Capacitive deionization
Selective phosphate removal
Layered double hydroxide hydroxide/
reduced graphene oxide composite

ABSTRACT

Phosphate removal is a critical issue in water treatment because excess levels of phosphate can cause severe eutrophication. Capacitive deionization (CDI), which has several advantages, such as simple, eco-friendly, and energy efficient operations, has gained attention as a potential alternative over conventional phosphate removal technologies like activated sludge, chemical precipitation, and adsorption processes. However, CDI suffers from a lack of selectivity for phosphate, resulting from non-selective anion removal of positively biased electrodes. Herein, the layered double hydroxide/reduced graphene oxide (LDH/rGO) composite electrode in the CDI process was examined for selective phosphate removal. LDH/rGO showed the selective phosphate removal performance with sustained phosphate removal efficiency even in the presence of excess chloride. In addition, the selective phosphate removal in the CDI process with the LDH/rGO was successfully demonstrated in the simulated water, fabricated by adding a significantly low concentration of phosphate (0.4 mg·L^{-1}) into real river water matrix (Han River,

* Corresponding author at: Korea Environment Institute, 370 Sicheong-daero, Sejong-si 30147, Republic of Korea.
E-mail address: jeyong@snu.ac.kr (J. Yoon).

https://doi.org/10.1016/j.jcis.2019.12.068
0021-9797/© 2019 Elsevier Inc. All rights reserved.

Seoul, Korea). This result was explained by the high electrochemical selectivity of the LDH/rGO for phosphate.

© 2019 Elsevier Inc. All rights reserved.

1. Introduction

A tremendous amount of phosphorus from various human activities, such as the use of pesticides, detergents, and manure, has been released into aquatic environments as a phosphate in wastewater. Excess levels of phosphate in water environments causes ecological damage through the process of eutrophication, one of the most widespread global water quality problems, leading to substantial economic problems and latent risk to human health [1,2]. For instance, the potential economic damage from eutrophication was estimated to be about $105–106 million annually in England and Wales, and even reached over $2.2 billion annually in the United States [3,4].

In order to control the phosphate concentration in discharge water, various technologies including chemical precipitation, activated sludge, and adsorption processes have been studied. However, chemical precipitation and activated sludge suffer from a sludge disposal problem, and adsorption process is limited by regeneration issue associated with the usage of a large amount of chemicals. Capacitive deionization (CDI) has been considered an alternative technology due to its eco-friendly, energy efficient, and simple operation based on charging/discharging [5–11]. In a conventional CDI process, ions can be captured from an aqueous phase by a simple electrostatic interaction between ions and electrode surface through the electrical double layer (EDL) formation on the electrode surface. It indicates that CDI has been suffered from selective phosphate removal, even though the selectivity should be considered in real applications. For this reason, developing a new approach for selective phosphate removal in CDI process is necessary [12–17].

This study examines a novel electrode material, the ZnAl-layered double hydroxide with reduced graphene oxide (LDH/rGO), for selective phosphate removal in the CDI process. Regarding selective property toward phosphate, ZnAl- LDH is one of good candidate material as a phosphate selective electrode in the CDI process [18,19]. However, the electrochemical application of ZnAl-LDH has been focused on the energy storage system [20,21]. In here, The morphology and electrochemical properties of the LDH/rGO were investigated in order to understand its phosphate capturing behavior. The phosphate selective removal performance of the LDH/rGO was examined under various ratios of phosphate to chloride (1:5, 1:10, and 1:20), considering energy consumption and regeneration practice. In addition, the phosphate removal performance of the LDH/rGO was examined in the real water matrix (Han River, Seoul, Korea) with adding a low level of phosphate (0.4 mg•L^{-1}). To best of our knowledge, it is the first report to intensively demonstrate the performance of electrochemical phosphate removal using LDH in various concentrations of a competing ion and the real water system.

2. Materials and method

2.1. 3. Reagents and chemicals

All chemicals were purchased from Sigma Aldrich (St. Louis, MO, USA), and used without further purification. The cation exchange membrane (Selemion® CMV, Asahi Glass Company, Japan) was used as received.

2.2. Preparation of composite electrode

The LDH/rGO powder was fabricated by following procedure [22]. First, for the preparation of the LDH/rGO powder as active material, rGO was synthesized using Hummers method [23]. Graphene oxide (GO) powder was immersed in 30 g•L^{-1} of L-ascorbic acid at 90 °C overnight. Then, the resulting rGO was well washed in deionized water and was dispersed in 250 mL of the aqueous solution which contained 0.744, 0.479, and 0.526 g of Zn$(NO_3)_2{\cdot}6H_2O$, Al$(NO_3)_3{\cdot}9H_2O$ and urea, respectively. The LDH/rGO powder was obtained by hydrothermal processing at 95 °C for 24 h.

Prior to fabrication of the LDH/rGO as a freestanding composite electrode, the LDH/rGO powder, conducting agent, and polytetrafluoroethylene (PTFE) were each mixed with weight ratios of 8:1:1. Then, the composite electrode was fabricated by the role-pressing method and dried in a vacuum oven. The pure LDH electrode, without adding rGO, was prepared with the same procedure.

2.3. Characterization of LDH/rGO

The LDH/rGO and the pure LDH powders were analyzed with a scanning electron microscope (SEM, JSM-6700F, Jeol, Tokyo, Japan), high resolution transmission electron microscope (HR-TEM, JEM 3010, Jeol, Tokyo, Japan), and X-ray diffractometer (XRD, the Rigaku D-MAX2500, Tokyo, Japan). Additionally, the LDH/rGO was examined by post-mortem analysis with Fourier Transform Infrared Spectroscopy (FT-IR, Cary 600 series FT-IR Agilent Technologies, CA, USA) and XRD analysis after capturing step. For XRD analysis, the capturing step was conducted under a high phosphate concentration (1 M of phosphate) to maximize changes for clear observation.

The electrochemical properties of the LDH/rGO were investigated using cyclic voltammetry (CV) and galvanostatic charge/discharge measurements. These measurements were conducted in a custom-built cell with installation of the LDH/rGO as a working electrode and excess activated carbon as a counter electrode [9]. With Ag/AgCl (saturated KCl) reference electrode, CV was performed in the three electrode system under 2 mV•s^{-1} in of phosphate solution (1 M, sodium phosphate) and chloride solution (1 M, sodium chloride) at a neutral pH, using a potentiostat (PARSTAT 2273, Princeton Applied Research, TN, USA). The galvanostatic charge/discharge was carried out using a battery cycler (WBCS3000, WonA Tech Co, Seoul, Korea) with/without Ag/AgCl (saturated KCl) reference electrode for monitoring potentials of the LDH/rGO.

2.4. Evaluation of LDH/rGO in CDI process for phosphate removal

The semi-batch electrochemical system was prepared with the LDH/rGO as a phosphate capturing electrode, and the nickel hexacyanoferrate (one of the Prussian blue analogues, PB) [24] with a cation exchange membrane as cation capturing electrode. Phosphate removal performance was tested in phosphate and chloride mixed solution at neutral. Phosphate concentration was 1 mM, and chloride concentration was varied from 5 mM to 20 mM.

Before the phosphate removal test, the PB was pretreated by applying a constant current of 0.6 mA•cm^{-2} until −1.5 V of the cell potential in 100 mM of potassium nitrate for the activation of PB by releasing cations. The phosphate removal by the LDH/rGO in

the CDI process was conducted by repeating the two steps up to the 5th cycle inducing electrochemical capturing and release of phosphate. For the capturing step, constant current (0.6 mA·cm^{-2}) with the cell voltage limit of 1.0 V was applied the system with the mixed solution containing 1 mM of phosphate and various concentrations of chloride ranging from 5 mM to 20 mM at neutral pH. In the releasing step, reverse current (−0.6 mA·cm^{-2}) was applied up to −1.5 V of the cell potential in the 10 mM of sodium hydroxide solution. The average values of removal efficiency for phosphate and chloride were estimated from where the process was stabilized. In addition, to express the selective performance of LDH/rGO in the CDI process, the selectivity coefficient (S) was also calculated as follows [25].

$$\text{Selectivity coefficient } (S) = \frac{R_P/C_P}{R_{Cl}/C_{Cl}} \quad (1)$$

where C_P (mmol·g^{-1}) and C_{Cl} (mmol·g^{-1}) were the amount of captured phosphate and chloride on the electrode, respectively, and R_P (mmol·L^{-1}) and R_{Cl} (mmol·L^{-1}) were the remaining aqueous concentrations of phosphate and chloride after the capturing step, respectively. Note that the R_p/C_p (L·g^{-1}) and R_{Cl}/C_{Cl} (L·g^{-1}) were the distribution coefficients for phosphate and chloride, respectively.

Energy consumption was calculated based on the area of cell potential vs. charge plot for capturing/releasing steps [26]. The samples were collected when the capturing or releasing step was finished, and the ion concentrations were measured with ion chromatography (DX-120, DIONEX, CA, USA). A carbon electrode (SX-plus, Norit Activated Carbon, Amersfoort, Netherland) was examined for comparative purposes under the selected condition (1 mM of phosphate and 10 mM of chloride solution).

Instead of 10 mM of sodium hydroxide solution in the releasing step, two different solutions (10 mM of sodium bicarbonate and 10 mM of sodium chloride) were examined. Capturing-releasing steps were repeated at a selected condition (1 mM of phosphate and 10 mM of chloride). From the 1st cycle to 3rd cycle, bicarbonate solution was used. From 4th cycle to 6th cycle, chloride solution was used.

2.5. Preparation of simulated water using real water matrix

The selective phosphate removal of the LDH/rGO in CDI process was examined in the simulated water (Han River, Seoul, Korea), which was prepared by adding 0.4 mg·L^{-1} of phosphate into the Han River water (micro filtered). The phosphate removal of LDH/rGO was evaluated in the CDI process by repeating capturing/releasing steps. 10 mM of sodium hydroxide solution was used for the releasing step.

3. Results and discussion

3.1. Characterization of LDH/rGO

Fig. 1 shows the XRD patterns (a), the SEM (b) and the TEM images (c) of the LDH/rGO in comparison with those of the pure LDH, respectively. As shown in Fig. 1(a), the LDH/rGO was successfully synthesized with a typical lamella structure of LDHs, which is confirmed by the identical peak positions of (0 0 3), (0 0 6), (0 0 9), (1 0 4) and (1 0 5) with pure LDH. However, in Fig. 1(b), a well-stacked structure was observed only for pure LDH by SEM image, while it was not clearly shown in the SEM image of the LDH/rGO, indicating that the layered structure was less developed. Considering the poor electrochemical properties of pure LDH due to large inter-layer distance, the less developed layered structure of the LDH/rGO appeared to be superior to pure LDH in terms of electrochemical properties due to a shorter inter-layer distance [27,28]. Furthermore, the TEM images of the LDH/rGO in Fig. 1(c) exhibited a graphene layer of the LDH/rGO, while no graphene layer was observed in case of the pure LDH. This graphene layer was also confirmed by AFM image of rGO showing similar wrinkled morphology (see Fig. S1 in Supplementary Information, SI). The graphene layer of the LDH/rGO is presumed to play a role as a conducting substrate leading to improvement in the conductive property of the LDH [27]. The structural advantages of LDH/rGO was supported by a larger area of the CV curve compared to that of pure LDH, indicating the improved electrochemical properties (refer to Fig. S2).

3.2. Phosphate selective properties of LDH/rGO

The phosphate removal properties of the LDH/rGO were examined with the CV curves (a), galvanostatic charge/discharging curves (b) The phosphate captured LDH/rGO was analyzed by FT-IR (c) and XRD (d) as shown in Fig. 2. In Fig. 2(a), the broad peaks with a red arrow appeared within the potential range from −0.4 V to 0.05 V (vs. Ag/AgCl) in the phosphate solution (1 M), while these peaks were not observed in the chloride solution (1 M). This result implies that LDH/rGO revealed the electrochemical reactions with phosphate, which can be interpreted by b-values of power-law relation for anodic and cathodic processes (0.8 and 0.9, respectively) (refer to Fig. S3(a) and (b) in SI).

As shown in Fig. 2(b), the electron transfer reaction of the LDH/rGO for phosphate was also displayed in the non-linear potential profile of the LDH/rGO. The slope of the potential profile for phosphate was changed near 0 V for anodic process and −0.2 V for cathodic process, leading to the higher specific capacity for phosphate when compared to chloride [29–31]. Additionally, the LDH/rGO electrode exhibited high cyclability in the phosphate solution with coulombic efficiency near unity and retained 71% of the initial discharge capacity after 100 cycles (refer to Fig. S4).

The electrochemical behavior of the LDH/rGO for phosphate can be explained by the inner-sphere complexation (Fig. 2(c)) and anion intercalation (Fig. 2(d)) of phosphate and the LDH/rGO. As shown in Fig. 2(c), the occurrence of inner-sphere complexation was observed by P—O stretching vibration peak around 1000 cm^{-1} after capturing step resulting from the formation of mono/bidentate complexes [32,33]. In the XRD pattern of Fig. 2 (d), new peaks appeared at higher 2 theta degree of (0 0 3) and (0 0 6), respectively, after capturing phosphate, which indicates that phosphate was intercalated into an interlayer of LDH with decreasing interlayer distance [33,34]. Additionally, based on XPS analysis, Zn and Al metal cations in LDH/rGO played role of adsorption sites (refer to Fig. S5).

3.3. Phosphate removal performance of LDH/rGO in the CDI process

The phosphate removal performance of LDH/rGO was evaluated in the CDI process under chloride-rich conditions. Fig. 3(a) displays the normalized ion concentration profile of the mixed solution of phosphate (1 mM) and chloride (10 mM) (refer to Fig. S6 in SI for the specific ion capacity (mmol·g^{-1})) during the capturing step. As shown in Fig. 3(a), the LDH/rGO exhibited selective removal behavior for phosphate during the capturing step, leading to a decrease in normalized phosphate concentration. This result corresponds well with the CV curve in Fig. 2(a), indicating the phosphate-selective nature of the LDH/rGO in an electrochemical process.

Fig. 3(b) shows the S value (selectivity coefficient, Eq. (1)) of chloride and phosphate, and their corresponding ion removal ratio at various concentrations of mixture solution. Note that when S value is greater than 1, the phosphate removal is favorable,

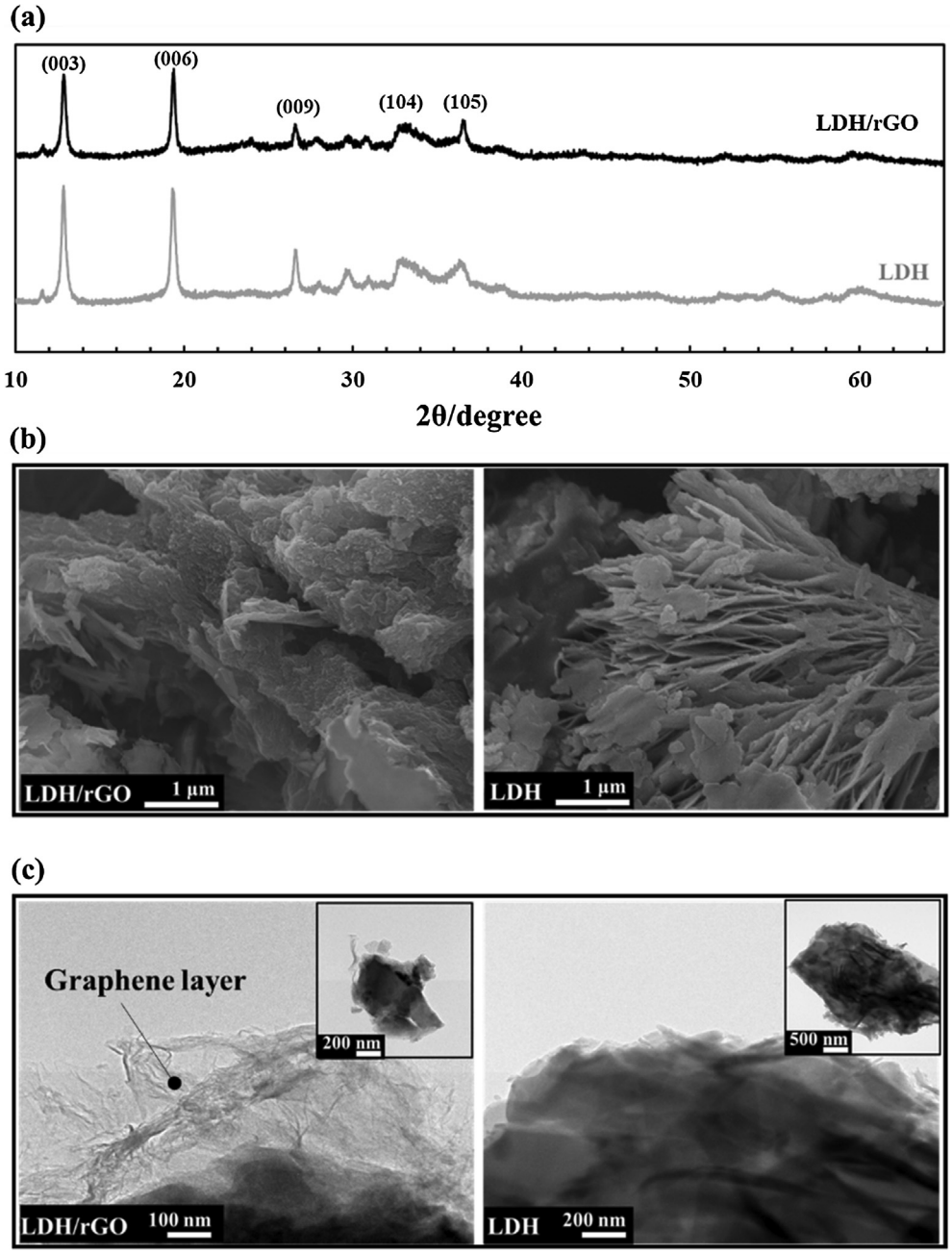


Fig. 1. XRD patterns (a), SEM images (b), TEM images (c) of layered double hydroxide/reduced graphene oxide composite (LDH/rGO) in comparison with those of pure layered double hydroxide as a powder form.

compared with the chloride removal at the selected condition. As shown in Fig. 3(b), the *S* value increased from 2.9 to 7.4 with increase of chloride concentration, indicating the phosphate selective property of LDH/rGO in the CDI process; the selective property of LDH/rGO is superior to that of the activated carbon electrode. Note that the *S* value of activated carbon was only 2.0 while the *S* value of the LDH/rGO was 6.1 at the selected condition (1 mM of phosphate and 10 mM of chloride). The high *S* value of LDH/rGO was attributed to the maintained significant phosphate removal, which decreased only from 54% to 48% even as the chloride concentration of mixture solution increased from 5 mM to 20 mM. Regarding the *S* value of rGO (~2.6) at 1 mM of phosphate and 10 mM of chloride mixed solution, LDH is thought to have a fundamental role to selective removal of phosphate while rGO is supporting material to enhance the electrochemical activity of LDH (refer to Fig. S7). Furthermore, the phosphate selective behavior was observed at various pH conditions, from pH 5 (major species is monovalent phosphate) to pH 8 (major spices is divalent phosphate), indicating that the synthesized LDH/rGO exhibited good selectivity for both divalent and monovalent phosphate forms (refer to Fig. S8) [33,35]. The selective property of LDH/rGO in the CDI process can be explained by the synergetic effect of LDH and rGO. When a positive potential is applied, LDH/rGO is polarized due to enhanced electrical conductivity as shown in Fig. S2. As a result, the electron density of transition metal sites is reduced leading that phosphate can easily make the inner-sphere complexation via a ligand exchange reaction [36].

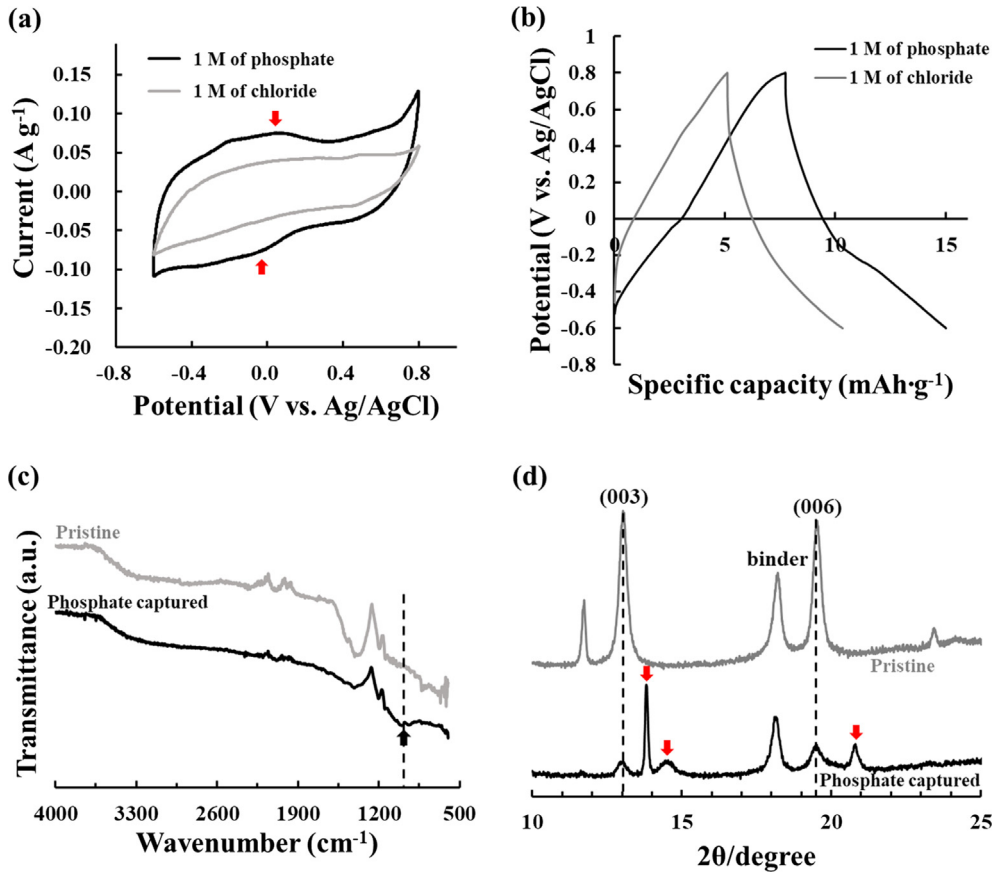


Fig. 2. Cyclic voltammograms (a) and galvanostatic charge/discharge curves (b) of layered double hydroxide/reduced graphene oxide (LDH/rGO) composite electrode in phosphate (1 M) and chloride solution (1 M), and the FT-IR spectra (c) and the XRD patterns (d) of pristine and phosphate captured (after capturing step) LDH/rGO. The FT-IR was conducted with the phosphate captured LDH/rGO prepared in 1 mM of phosphate and 5 mM of chloride, and the XRD was measured with the phosphate captured LDH/rGO prepared in 1 M of phosphate solution.

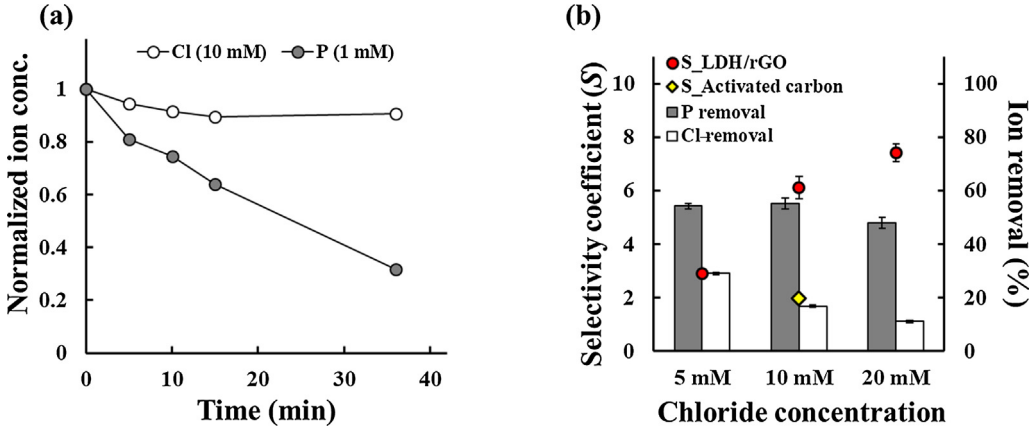


Fig. 3. The normalized ion concentration profile during the capturing step in the mixture solution (1 mM phosphate and 10 mM chloride) (a), and the selectivity coefficient (*S*) of layered double hydroxide/reduced graphene oxide (LDH/rGO) composite electrode in the capacitive deionization (CDI) process (b). The mixed solution was used for capturing step in (b) consisted of 1 mM of phosphate and various concentration of chloride. For the releasing step, 10 mM of sodium hydroxide was used as an electrolyte. The *S* value of activated carbon electrode was also displayed in (b) for the comparison (yellow diamond mark). (For interpretation of the references to colour in this figure legend, the reader is referred to the web version of this article.)

3.4. Energy consumption

The energy consumption of the CDI process using the LDH/rGO was estimated from the area of cell potential profiles vs. charge shown in Fig. 4. As shown in Fig. 4, the energy consumptions were calculated as 176, 163, and 168 Wh·m^{-3} for the range of 45–55% phosphate removal under three different conditions (5 mM, 10 mM, and 20 mM of chloride with 1 mM of phosphate, respectively). Higher energy consumption in the case of 5 mM of chloride mixture solution (1 mM of phosphate) was caused by higher solution resistance, which was reflected as a higher cell potential profile during the capturing step (Fig. 4). The energy consumption

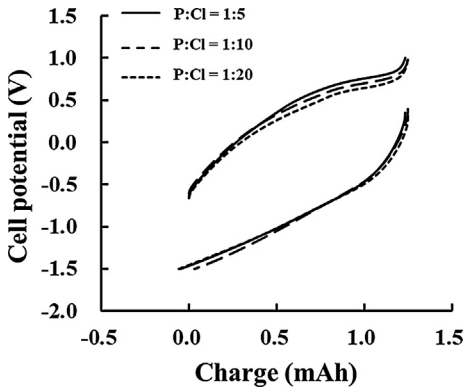


Fig. 4. The cell potential vs. charge curves under three different conditions (5, 10, 20 mM of chloride, respectively, with 1 mM of phosphate). Note that the area of the cell potential vs. charge curves indicates the energy consumption for each condition.

of the LDH/rGO in the CDI process was small compared to the energy consumption of electrocoagulation process (410–22,000 Wh·m^{-3} with 22–100% removal of phosphate) [37].

3.5. Examination of several regeneration solutions during releasing step

Fig. 5 displays the *S* value of LDH/rGO in the CDI process at two different regeneration solutions for the releasing step. Bicarbonate and chloride solutions were selected because they are more environmentally benign chemicals than hydroxide solution. Sodium bicarbonate (10 mM) was used as a regeneration solution up to 3th cycle, and sodium chloride (10 mM) was used from 4th cycle to 6th cycle. Although the phosphate removal efficiency gradually decreased with the use of bicarbonate and chloride solutions, the phosphate selective performance showing the *S* value above 4.0 was still observed.

3.6. Application of LDH/rGO in the simulated real water matrix

Fig. 6 presents the phosphate removal performance of LDH/rGO in the capacitive deionization (CDI) process in the simulated water which was prepared by adding about 0.4 mg·L^{-1} of phosphate into

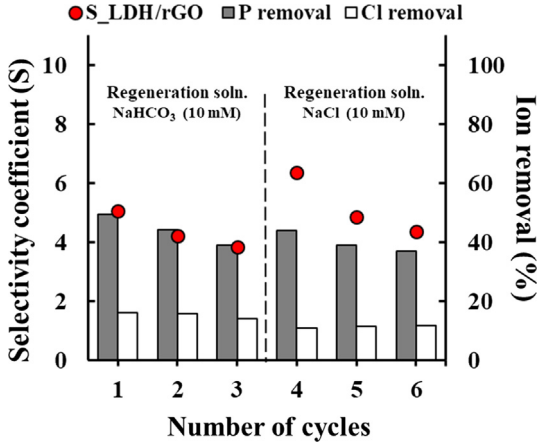


Fig. 5. The selectivity coefficient (*S*) of layered double hydroxide/reduced graphene oxide (LDH/rGO) composite electrode measured in different regeneration solutions (sodium bicarbonate and sodium chloride). For all capturing steps from 1st cycle to 6th cycle, the mixed solution of phosphate (1 mM) and chloride (10 mM) was used. The releasing step was conducted with sodium bicarbonate (10 mM, pH 8.5, from 1st cycle to 3th cycle), and sodium chloride (10 mM, pH 7.2, from 4th cycle to 6th cycle).

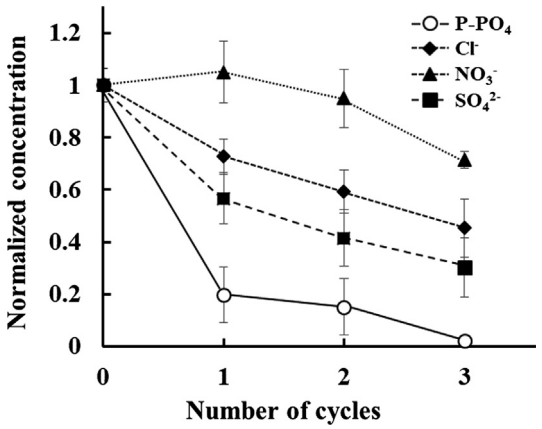


Fig. 6. Phosphate removal from the real simulated water matrix (Han River, Seoul, Korea) via layered double hydroxide/reduced graphene oxide (LDH/rGO) composite electrode in the capacitive deionization (CDI) process. 0.4 mg·L^{-1} of phosphate was added in the real water matrix. In the releasing step, 10 mM of sodium hydroxide solution was used.

Table 1
Anion composition of Han River water (Korea).

Anions (pH 8.1)	Concentration [mg·L^{-1}, (mM)]	Concentration Ratio [mole of anions/mole of P·PO$_4$]
PO_4^{3-}(added)	0.38 (0.012)	1
Cl^-	32 (0.91)	76
NO_3^-	15.5 (0.25)	21
SO_4^{2-}	18.9 (0.20)	17

Han River water (Seoul, Korea, refer to Table 1 for anion composition). As an example, this phosphate concentration is similar to the wastewater treatment plant in Goyang, Korea. As shown in Fig. 6, in spite of very low phosphate concentration in the real water matrix, the LDH/rGO successfully achieved the selective phosphate removal. The concentration of phosphate was decreased from 0.4 mg·L^{-1} to 0.009 mg·L^{-1} (the target concentration of phosphate of waste water treatment plant: 0.1 mg·L^{-1}). This was about 98% removal, while the removal efficiency of other anions was 55%, 28%, and 70% for Cl^-, NO_3^-, and SO_4^{2-}, respectively. These results suggest the LDH/rGO has an excellent selective phosphate removal performance, as compared to other anion species in real water matrix. Therefore, the selective property of LDH/rGO in the CDI process was well demonstrated in the study with a moderate value of phosphate adsorption capacity compared to other studies (refer to Table S1).

4. Conclusion

In this study, the phosphate selective removal of LDH/rGO was successfully demonstrated in the CDI process. With repeated capturing and release, the selective removal performance of LDH/rGO was sustained even when the chloride concentration was increased to 20 times higher than phosphate concentration. This phosphate selective performance of the LDH/rGO was also demonstrated by its high *S* value compared to activated carbon electrode (6.1 for LDH/rGO, and 2.0 for activated carbon electrode). In addition, the LDH/rGO in the CDI process exhibited good energy efficiency and reusability. Furthermore, phosphate in the real water matrix (Han River, Seoul, Korea) was selectively removed by the LDH/rGO in the CDI process. This result is explained by the high electrochemical selectivity of the LDH/rGO for phosphate.

CRediT authorship contribution statement

Sung Pil Hong: Conceptualization, Writing - original draft, Investigation. **Hansun Yoon:** Investigation. **Jaehan Lee:** Resources. **Choonsoo Kim:** Writing - review & editing. **Seoni Kim:** Validation. **Jiho Lee:** Investigation, Writing - review & editing. **Changha Lee:** Writing - review & editing. **Jeyong Yoon:** Supervision.

Declaration of Competing Interest

The authors declare that they have no known competing financial interests or personal relationships that could have appeared to influence the work reported in this paper.

Acknowledgement

This work was supported by the Technology Innovation Program (10082572, Development of Low Energy Desalination Water Treatment Engineering Package System for Industrial Recycle Water Production) funded by the Ministry of Trade, Industry and Energy, South Korea (MOTIE, Korea), and the National Research Foundation of Korea (NRF) grant funded by the Korea government (MSIT), South Korea (NRF-2019R1G1A1003336).

Appendix A. Supplementary material

Supplementary data to this article can be found online at https://doi.org/10.1016/j.jcis.2019.12.068.

References

[1] B.K. Mayer, L.A. Baker, T.H. Boyer, P. Drechsel, M. Gifford, M.A. Hanjra, P. Parameswaran, J. Stoltzfus, P. Westerhoff, B.E. Rittmann, Total value of phosphorus recovery, Environ. Sci. Technol. 50 (13) (2016) 6606–6620.
[2] Y. Gu, D. Xie, Y. Ma, W. Qin, H. Zhang, G. Wang, Y. Zhang, H. Zhao, Size modulation of zirconium-based metal organic frameworks for highly efficient phosphate remediation, ACS Appl. Mater. Interfaces 9 (37) (2017) 32151–32160.
[3] W.K. Dodds, W.W. Bouska, J.L. Eitzmann, T.J. Pilger, K.L. Pitts, A.J. Riley, J.T. Schloesser, D.J. Thornbrugh, Eutrophication of U.S. freshwaters: analysis of potential economic damages, Environ. Sci. Technol. 43 (1) (2009) 12–19.
[4] J.N. Pretty, C.F. Mason, D.B. Nedwell, R.E. Hine, S. Leaf, R. Dils, Environmental costs of freshwater eutrophication in England and Wales, ACS Publications, 2003.
[5] C. Kim, J. Lee, S. Kim, J. Yoon, TiO_2 sol–gel spray method for carbon electrode fabrication to enhance desalination efficiency of capacitive deionization, Desalination 342 (2014) 70–74.
[6] T. Kim, J. Dykstra, S. Porada, A. Van der Wal, J. Yoon, P. Biesheuvel, Enhanced energy and charge efficiencies by increasing the discharge voltage in capacitive deionization, J. Colloid Interface Sci. 446 (2015) 317–326.
[7] C. Kim, J. Lee, P. Srimuk, M. Aslan, V. Presser, Concentration-gradient multichannel flow-stream membrane capacitive deionization cell for high desalination capacity of carbon electrodes, ChemSusChem 10 (24) (2017) 4914–4920.
[8] H. Yoon, J. Lee, S. Kim, J. Yoon, Review of concepts and applications of electrochemical ion separation (EIONS) process, Sep. Purif. Technol. 215 (2019) 190–207.
[9] J. Lee, S. Kim, J. Yoon, Rocking chair desalination battery based on prussian blue electrodes, ACS Omega 2 (4) (2017) 1653–1659.
[10] J. Lee, S. Kim, C. Kim, J. Yoon, Hybrid capacitive deionization to enhance the desalination performance of capacitive techniques, Energy Environ. Sci. 7 (11) (2014) 3683–3689.
[11] S. Kim, H. Yoon, D. Shin, J. Lee, J. Yoon, Electrochemical selective ion separation in capacitive deionization with sodium manganese oxide, J. Colloid Interface Sci. 506 (2017) 644–648.
[12] X. Huang, D. He, W. Tang, P. Kovalsky, T.D. Waite, Investigation of pH-dependent phosphate removal from wastewaters by membrane capacitive deionization (MCDI), Environ. Sci. Water Res. Technol. 3 (5) (2017) 875–882.
[13] C. Macías, P. Lavela, G. Rasines, M.C. Zafra, J.L. Tirado, C.O. Ania, Improved electro-assisted removal of phosphates and nitrates using mesoporous carbon aerogels with controlled porosity, J. Appl. Electrochem. 44 (8) (2014) 963–976.
[14] M.C. Zafra, P. Lavela, C. Macías, G. Rasines, J.L. Tirado, Electrosorption of environmental concerning anions on a highly porous carbon aerogel, J. Electroanal. Chem. 708 (2013) 80–86.
[15] J.C. Farmer, D.V. Fix, G.V. Mack, R.W. Pekala, J.F. Poco, Capacitive, Deionization with Carbon Aerogel Electrodes: Carbonate, Sulfate, and Phosphate, Lawrence Livermore National Lab, 1995.
[16] Z. Ge, X. Chen, X. Huang, Z.J. Ren, Capacitive deionization for nutrient recovery from wastewater with disinfection capability, Environ. Sci. Water Res. Technol. 4 (1) (2018) 33–39.
[17] Z. Chen, H. Zhang, C. Wu, Y. Wang, W. Li, A study of electrosorption selectivity of anions by activated carbon electrodes in capacitive deionization, Desalination 369 (2015) 46–50.
[18] E.M. Seftel, R.G. Ciocarlan, B. Michielsen, V. Meynen, S. Mullens, P. Cool, Insights into phosphate adsorption behavior on structurally modified ZnAl layered double hydroxides, Appl. Clay Sci. 165 (2018) 234–246.
[19] H. He, H. Kang, S. Ma, Y. Bai, X. Yang, High adsorption selectivity of ZnAl layered double hydroxides and the calcined materials toward phosphate, J. Colloid Interface Sci. 343 (1) (2010) 225–231.
[20] X. Chen, Z. Yang, L. Wang, H. Qin, Synthesis of rose-like ZnAl-LDH and its application in zinc-nickel secondary battery, Nanotechnology 30 (1) (2019) 015602.
[21] L. Liu, M. Cheng, Z. Yang, Improved performance of flower-like ZnAl LDH growing on carbon nanotubes used in zinc–nickel secondary battery, Electrochim. Acta 277 (2018) 67–76.
[22] Z. Gao, J. Wang, Z. Li, W. Yang, B. Wang, M. Hou, Y. He, Q. Liu, T. Mann, P. Yang, Graphene nanosheet/Ni2+/Al3+ layered double-hydroxide composite as a novel electrode for a supercapacitor, Chem. Mater. 23 (15) (2011) 3509–3516.
[23] W.S. Hummers Jr, R.E. Offeman, Preparation of graphitic oxide, J. Am. Chem. Soc. 80 (6) (1958). 1339-1339.
[24] H. Yoon, J. Lee, S. Kim, J. Yoon, Electrochemical sodium ion impurity removal system for producing high purity KCl, Hydrometallurgy 175 (2018) 354–358.
[25] X. Su, J. Hübner, M.J. Kauke, L. Dalbosco, J. Thomas, C.C. Gonzalez, E. Zhu, M. Franzreb, T.F. Jamison, T.A. Hatton, Redox interfaces for electrochemically controlled protein-surface interactions: bioseparations and heterogeneous enzyme catalysis, Chem. Mater. 29 (13) (2017) 5702–5712.
[26] S. Kim, J. Lee, J.S. Kang, K. Jo, S. Kim, Y.E. Sung, J. Yoon, Lithium recovery from brine using a lambda-MnO_2/activated carbon hybrid supercapacitor system, Chemosphere 125 (2015) 50–56.
[27] F. Song, X. Hu, Exfoliation of layered double hydroxides for enhanced oxygen evolution catalysis, Nat. Commun. 5 (2014) 4477.
[28] L. Sun, Y. Zhang, Y. Zhang, H. Si, W. Qin, Y. Zhang, Reduced graphene oxide nanosheet modified NiMn-LDH nanoflake arrays for high-performance supercapacitors, Chem. Commun. 54 (72) (2018) 10172–10175.
[29] H. Kim, J. Hong, Y.-U. Park, J. Kim, I. Hwang, K. Kang, Sodium storage behavior in natural graphite using ether-based electrolyte Systems, Adv. Funct. Mater. 25 (4) (2015) 534–541.
[30] T. Brousse, D. Bélanger, J.W. Long, To be or not to be pseudocapacitive?, J Electrochem. Soc. 162 (5) (2015) A5185–A5189.
[31] Y. Yang, L.C. Kao, Y. Liu, K. Sun, H. Yu, J. Guo, S.Y.H. Liou, M.R. Hoffmann, Cobalt-doped black TiO2 nanotube array as a stable anode for oxygen evolution and electrochemical wastewater treatment, ACS Catal. 8 (5) (2018) 4278–4287.
[32] K. Yang, L.-G. Yan, Y.-M. Yang, S.-J. Yu, R.-R. Shan, H.-Q. Yu, B.-C. Zhu, B. Du, Adsorptive removal of phosphate by Mg–Al and Zn–Al layered double hydroxides: kinetics, isotherms and mechanisms, Sep. Purif. Technol. 124 (2014) 36–42.
[33] K. Morimoto, S. Anraku, J. Hoshino, T. Yoneda, T. Sato, Surface complexation reactions of inorganic anions on hydrotalcite-like compounds, J. Colloid Interface Sci. 384 (1) (2012) 99–104.
[34] M. Khaldi, M. Badreddine, A. Legrouri, M. Chaouch, A. Barroug, A. De Roy, J.P. Besse, Preparation of a well-ordered layered nanocomposite from zinc–aluminum–chloride layered double hydroxide and hydrogenophosphate by ion exchange, Mater. Res. Bull. 33 (12) (1998) 1835–1843.
[35] F. Morel, J.G. Hering, J.G. Hering, Principles and Applications of Aquatic Chemistry, John Wiley & Sons, 1993.
[36] C.-L. Lin, M.-Y. Fang, S.-H. Cheng, Substituent and axial ligand effects on the electrochemistry of zinc porphyrins, J. Electroanal. Chem. 531 (2) (2002) 155–162.
[37] Ş. İrdemez, Y.Ş. Yildiz, V. Tosunoğlu, Optimization of phosphate removal from wastewater by electrocoagulation with aluminum plate electrodes, Sep. Purif. Technol. 52 (2) (2006) 394–401.